Supporting information

Three isomers in equilibrium: Phosphine exchange of coordinated and pendant phosphines in a unique complex, $(OC)_5WL$ (L = 1,2-bis(diphenylphosphino)-1-di-*p*-tolylphosphino-ethane). Implications for understanding the k_2 term in the rate law for phosphine substitution in group 6 metal carbonyl complexes.

Bret R. Van Ausdall,[†] Michael F. Cuddy,[‡] Joel S. Southern,[†] Kraig A. Wheeler,[§] Ellen A. Keiter,[†] Edward M. Treadwell,[†*] Richard L. Keiter.[†*⊥]

†Department of Chemistry, Eastern Illinois University, Charleston, Illinois 61920, United States
‡Department of Chemistry, Northwest College, Powell, Wyoming 82435, United States
§ Department of Chemistry, Whitworth University, Spokane, Washington 99251, United States

Table of Contents

1. Synthetic Scheme to Prepare Linkage Isomers 3a, 3b, and 3c

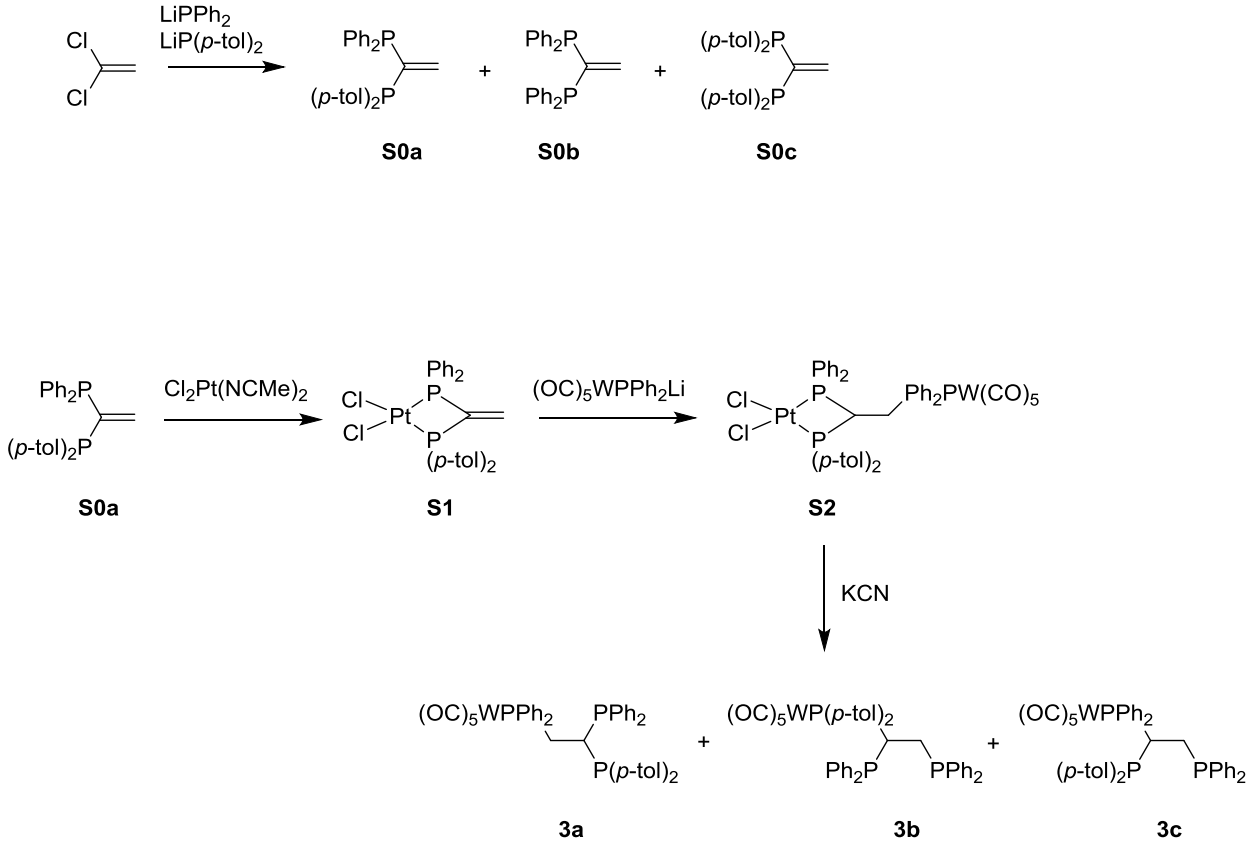

Spectroscopy

NMR data for the precursors leading to the three linkage isomers**,** $[(OC)_5W\{\kappa^1\text{-}P(p\text{-tol})_2\text{-}CH(PPh_2)CH_2PPh_2\}]$, $[(OC)_5W\{\kappa^1\text{-}PPh_2CH[P(p\text{-tol})_2]CH_2PPh_2\}]$ and $[(OC)_5W\{\kappa^1\text{-}PPh_2CH_2CH(PPh_2)[P(p\text{-tol})_2]\}]$

2. ^{31}P and ^1H NMR Data for $(Ph_2P)[(p\text{-tol})_2P]C{=}CH_2$

$^{31}P\{^1H\}$ NMR of $(Ph_2P)[(p\text{-tol})_2P]C{=}CH_2$, $(Ph_2P)_2C{=}CH_2$ and $[(p\text{-tol})_2P]_2C{=}CH_2$:

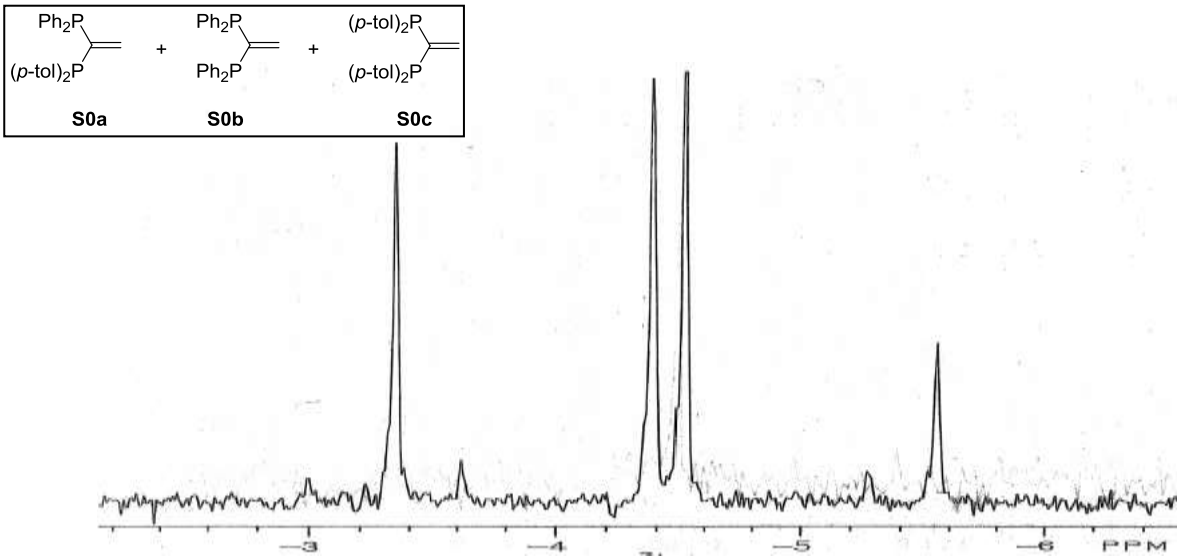

Figure S2.1. $^{31}P\ \{^1H\}$ NMR spectrum of a mixture of $(Ph_2P)_2C{=}CH_2$, $(Ph_2P)[(p\text{-tol})_2P]C{=}CH_2$, and $[(p\text{-tol})_2PC{=}CH_2]$. $(Ph_2P)_2C{=}CH_2$, δ-3.29; $(Ph_2P)[(p\text{-tol})_2P]C{=}CH_2$, AB spectrum: δ_{PPh2} -4.32, δ_{PPh2} -4.47, $^2J_{PP}$ 92.5; $[(p\text{-tol})_2PC{=}CH_2]$, δ-5.49.

Analysis of the (AB) portion of the ABXY spectrum of pure $(Ph_2P)\ [(p\text{-tol})_2P]C{=}CH_2$ gave δ_{PPh2} = -4.32 ppm, $\delta_{P(p\text{-tolyl})2}$ = -4.47 ppm, $^2J_{PP}$ = 92.5 Hz. Minor components, $(Ph_2P)_2C{=}CH_2$ and $[(p\text{-tol})_2P]_2C{=}CH_2$, observed in mixtures, gave signals at -3.29 ppm and -5.49 ppm, respectively.

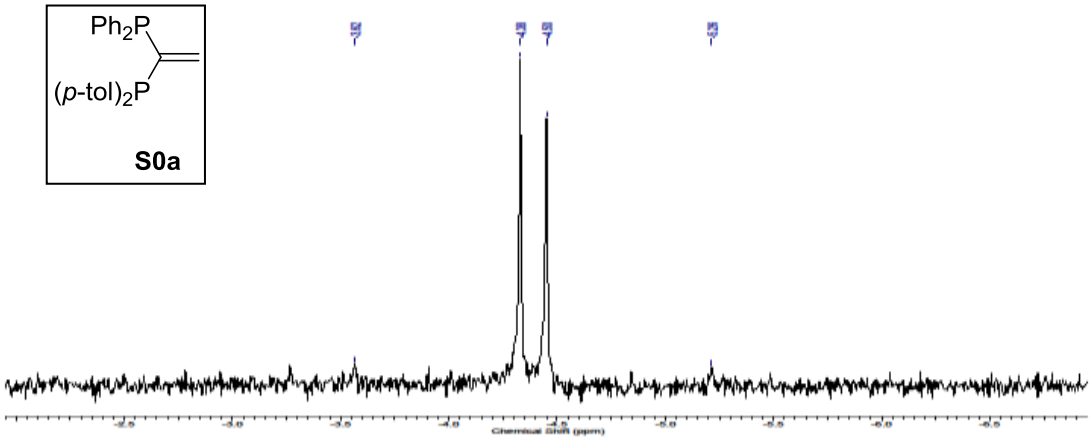

Figure S2.2. $^{31}P\ \{^1H\}$ NMR spectrum of isolated $(Ph_2P)[(p\text{-tol})_2P]C{=}CH_2$.

^{1}H NMR of (Ph$_2$P)[(*p*-tol)$_2$P]C=CH$_2$: The proton portion (XY) of the ABXY of the spectrum was analyzed as first-order, with each hydrogen atom giving rise to a doublet of doublet of doublets to give a total of 16 lines for the two hydrogen atoms. The H atom trans to Ph$_2$P is found at 5.81 ppm. $^3J_{PH(trans)}$ = 27 Hz; $^3J_{PH(cis)}$ = 12 Hz; $^2J_{HH'}$ = 1.5 Hz. The H atom trans to (*p*-tol)$_2$P is at 5.77 ppm. $^3J_{PH(trans)}$ = 28 Hz; $^3J_{PH(cis)}$ = 11.5 Hz; $^2J_{HH'}$ = 1.5 Hz.

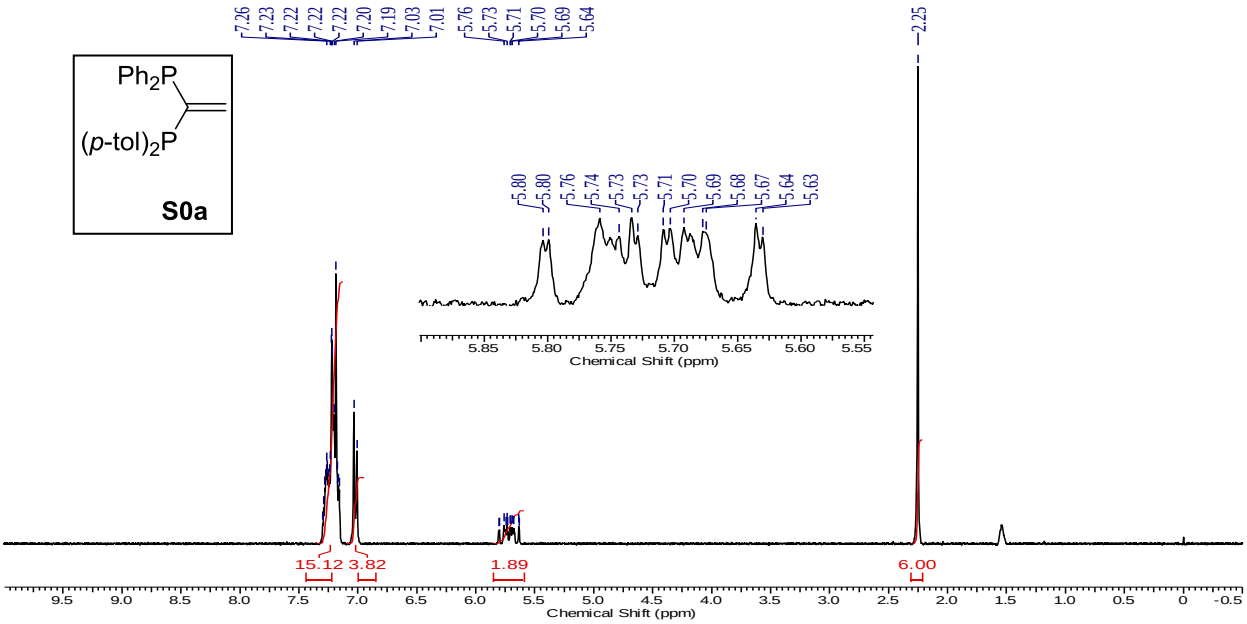

Figure S2.3. ^{1}H NMR spectrum of (Ph$_2$P)[(*p*-tol)$_2$P]C=CH$_2$. δ 5.81 (trans to Ph$_2$P-), $^3J_{HP(trans)}$ 27, $^3J_{HP(cis)}$ 12, $^2J_{HH}$ 1.5; δ 5.77 (trans to [(*p*-tol)$_2$P-], $^3J_{HP(trans)}$ 28, $^3J_{HP(cis)}$ 11.5, $^2J_{HH}$ 1.5; δ_{Me} 2.3; δ_{Ph} 6.9-7.4

3. ^{31}P and ^{1}H NMR Data for [Cl$_2$Pt{κ^2-(PPh$_2$)[P(*p*-tol)$_2$]C=CH$_2$}]

^{31}P{^{1}H} NMR of [Cl$_2$Pt{κ^2-(PPh$_2$)[P(*p*-tol)$_2$]C=CH$_2$}]:
δ_A = -31.52 ppm; δ_B = -32.55 ppm; $^2J_{P(A)P(B)}$ = 2 Hz; $^1J_{PtP(A)}$ = 3276 Hz, $^1J_{PtP(B)}$ = 3239 Hz

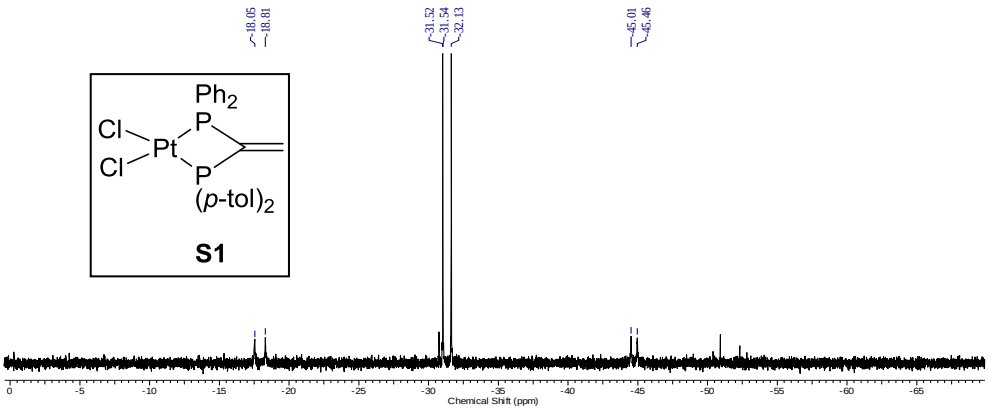

Figure S3.1. ^{31}P {^{1}H} NMR spectrum of [Cl$_2$Pt{κ^2-(Ph$_2$P$_a$)[(*p*-tol)$_2$P$_b$]C=CH$_2$}]. δ_a 31.52, δ_b 32.55, $^2J_{PP}$ 2, $^1J_{PtP(a)}$ 3276, $^1J_{PtP(b)}$ 3239.

^{1}H NMR of [Cl$_2$Pt{κ^2-(PPh$_2$)[P(*p*-tol)$_2$]C=CH$_2$}]: The proton portion (XY) of the ABXY of spectrum was analyzed as first-order, with each hydrogen atom giving rise to a doublet of doublet of doublets to give a total of 16 lines for the two hydrogen atoms. The H atom trans to Ph$_2$P is found at 6.30 ppm. $^3J_{PH(trans)}$ = 39 Hz; Hz; $^3J_{PH(cis)}$ = 25 Hz; $^2J_{HH'}$ = 1.5 Hz. The H atom trans to (*p*-tolyl)$_2$P is at 6.20 ppm. $^3J_{PH(trans)}$ = 28 Hz; $^3J_{PH(cis)}$ = 25 Hz; $^2J_{HH'}$ = 1.5 Hz. δ_{CH3} = 2.38 ppm.

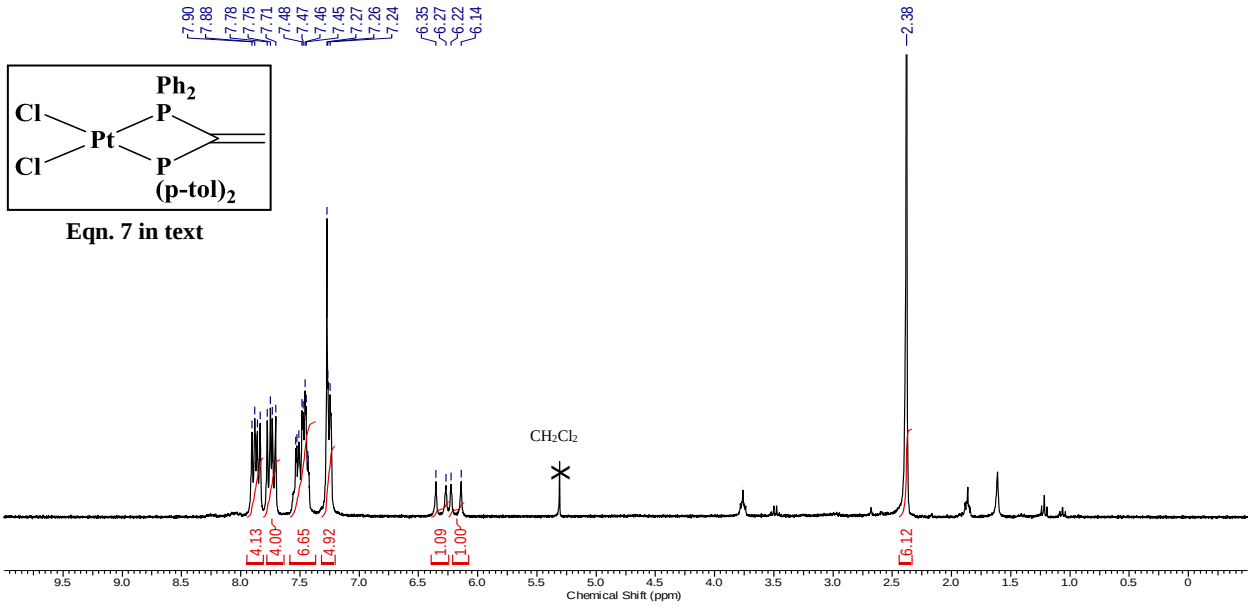

Figure S3.2. ^{1}H NMR spectrum of [Cl$_2$Pt{κ^2-(Ph$_2$P$_a$)[(*p*-tol)$_2$P$_b$]C=CH$_2$}]. δ 6.30 (trans to Ph$_2$P-), $^3J_{HP(trans)}$ 39, $^3J_{HP(cis)}$ 25, $^2J_{HH}$ 1.5; δ 6.20 (trans to [(*p*-tol)$_2$P-], $^3J_{HP(trans)}$ 28, $^3J_{HP(cis)}$ 25, δ_{Me} 2.39; δ_{Ph} 6.9-7.4.

4. ^{31}P NMR Data for [(OC)$_5$W{κ^1,κ^2-PPh$_2$CH$_2$CH[P(*p*-tol)$_2$](PPh$_2$)}PtCl$_2$]

^{31}P{^{1}H} NMR of (OC)$_5$WPPh$_2$CH$_2$CH(PPh$_2$)[P(*p*-tol)$_2$]PtCl$_2$: The ^{31}P spectrum is an example of an ABXKL spectrum in which A and B phosphorus atoms are bound to platinum (K), and X is bound to tungsten (L). The X portion will appear as a triplet if J_{AX} and J_{BX} are of the same (or nearly the same) magnitude as is true in our example. The AB portion of the spectrum consists of two pseudo-AB quartets, the total intensities of which are equal.

Tungsten region (X) δ_X = 22.10 ppm

It is not possible to determine J_{AX} or J_{BX} separately but the average ½($^3J_{(AX+BX)}$) = 5 Hz. This value is consistent with that found previously in (OC)$_5$WPPh$_2$CH$_2$CH(PPh$_2$)$_2$PtCl$_2$ for which $^3J_{PP}$ is 5 Hz and $^1J_{WP}$ = 251 Hz. In (OC)$_5$WPPh$_2$CH$_2$CH(PPh$_2$)[P(*p*-tol)$_2$]PtCl$_2$, a value of 246 Hz was found.

Platinum region (AB)

The AB portion ($^2J_{PP}$) of the spectrum presents the appearance of an AB quartet, each line of which is split into a doublet. It is tempting to take these doublet spacings as a measure of J_{AX} and J_{BX} . This is correct, however, only when J_{AX} = J_{BX}. While this is nearly true in this case, the spacings are best treated as ½($^3J_{(AX+BX)}$) to give a best value of 5 Hz.

$^2J_{PP}$ is given by the outer spacings of the pseudo-AB quartets. This spacing appears four times to give an average best value of 67 Hz.

The platinum-phosphorus coupling constants could not be determined with accuracy from this spectrum. Assuming that the most intense signal of the pseudo-quartets goes with the weak signal at -46.31 ppm, we have $^1J_{Pt\text{-}P}$ = 2922 Hz. This value is in the ballpark was shown by comparison to $(OC)_5WPPh_2CH_2CH(PPh_2)_2PtCl_2$ which has a value of 3027 Hz. There should, of course, be two Pt-P satellites but we were not able to sort things out from the low intensity signals.

The chemical shifts for the AB portion may be calculated from the equation

$$\Delta\nu = [(\nu_1 - \nu_4)(\nu_2 - \nu_3)]^{1/2}$$

$\delta_{PtP(Ph)}$ = 33.17 ppm; $\delta_{PtP(tol)}$ = 34.65 ppm

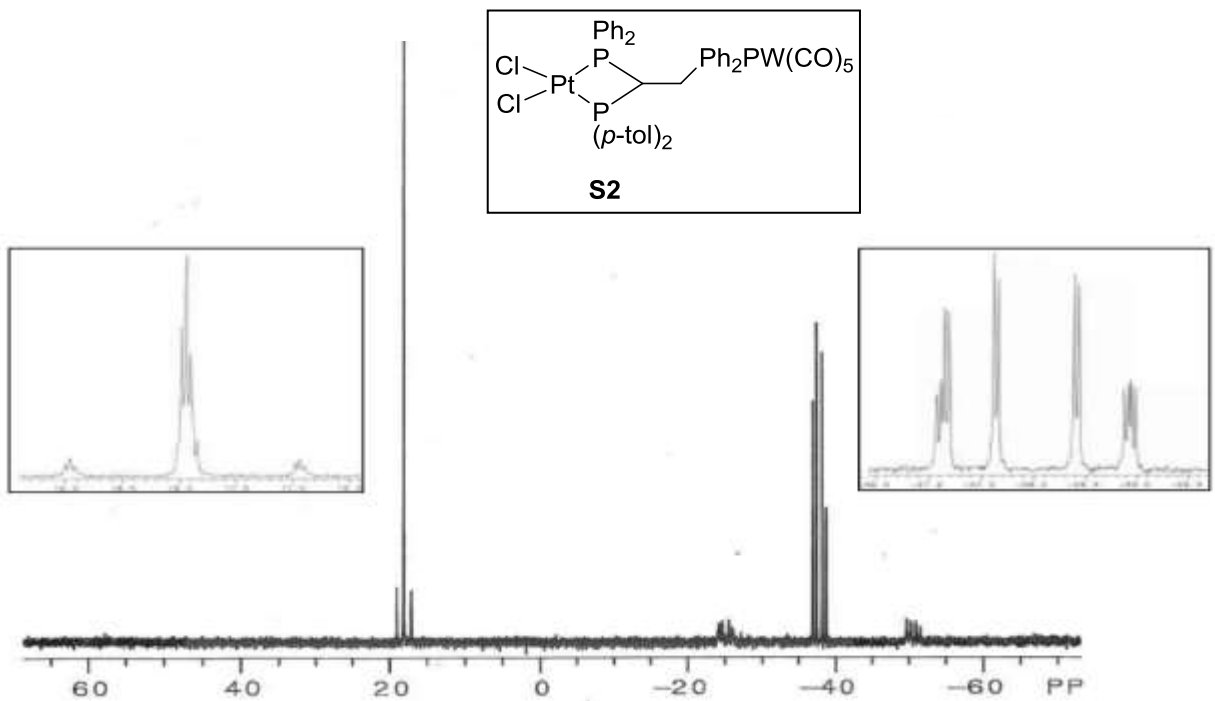

Figure S4.1. $^{31}P\{^1H\}$ NMR spectrum of $[(OC)_5W\{\kappa^1,\kappa^2\text{-}P_xPh_2CH_2CH[P_a(p\text{-tol})_2](P_bPh_2)\}PtCl_2]$. ABX spin system. $\delta_{P(x)}$ 22.10, ½($J_{[P(a)P(x) + P(b)(x)]}$) 5, $^1J_{WP}$ 246; $\delta_{P(b)}$ -33.17, δ_a -34.65, $^2J_{P(a)P(b)}$ 67, ½($J_{[P(a)P(x) + P(b)(x)]}$) 5, $^1J_{Pt(b)}$ 2932, $^1J_{Pt(a)}$ 3027.

5. ^{31}P, ^{1}H, and ^{13}C NMR Data for $[(OC)_5W\{\kappa^1\text{-}P(p\text{-tol})_2CH(PPh_2)CH_2PPh_2\}]$

$^{31}P\{^1H\}$ NMR of $[(OC)_5W\{\kappa^1\text{-}P(p\text{-tol})_2CH(PPh_2)CH_2PPh_2\}]$:

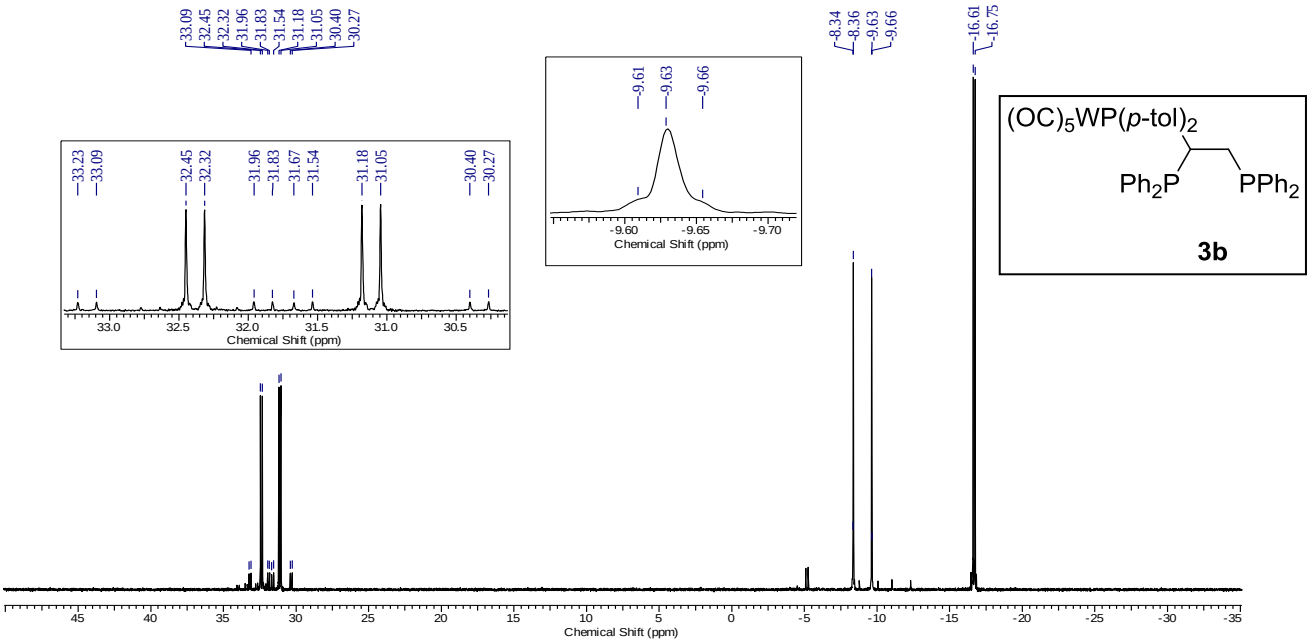

Figure S5.1. $^{31}P\{^1H\}$ NMR spectrum of $[(OC)_5W\{\kappa^1\text{-}P(p\text{-tol})_2CH(PPh_2)CH_2PPh_2\}]$ **3b**.

^{1}H NMR of $[(OC)_5W\{\kappa^1\text{-}P(p\text{-tol})_2CH(PPh_2)CH_2PPh_2\}]$:

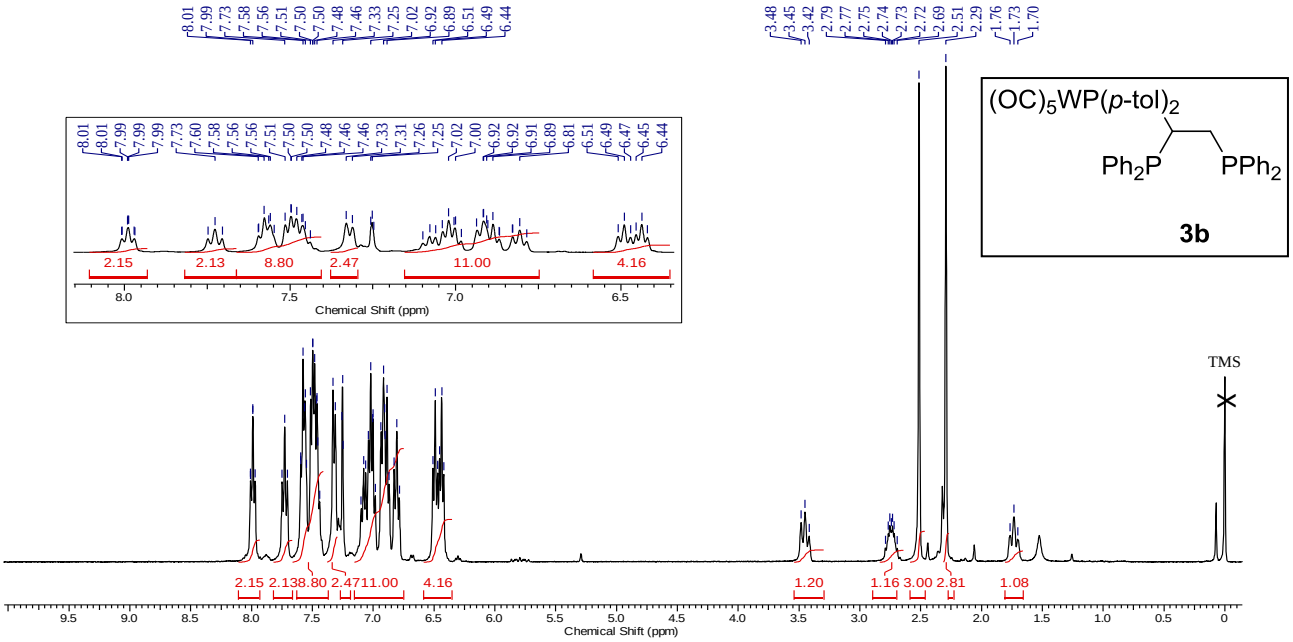

Figure S5.2. ^{1}H NMR spectrum of $[(OC)_5W\{\kappa^1\text{-}P(p\text{-tol})_2CH(PPh_2)CH_2PPh_2\}]$ **3b**. Diastereotopic methyl and methylene groups.

$^{13}C\{^1H\}$ NMR of $[(OC)_5W\{\kappa^1\text{-}P(p\text{-tol})_2CH(PPh_2)CH_2PPh_2]$:

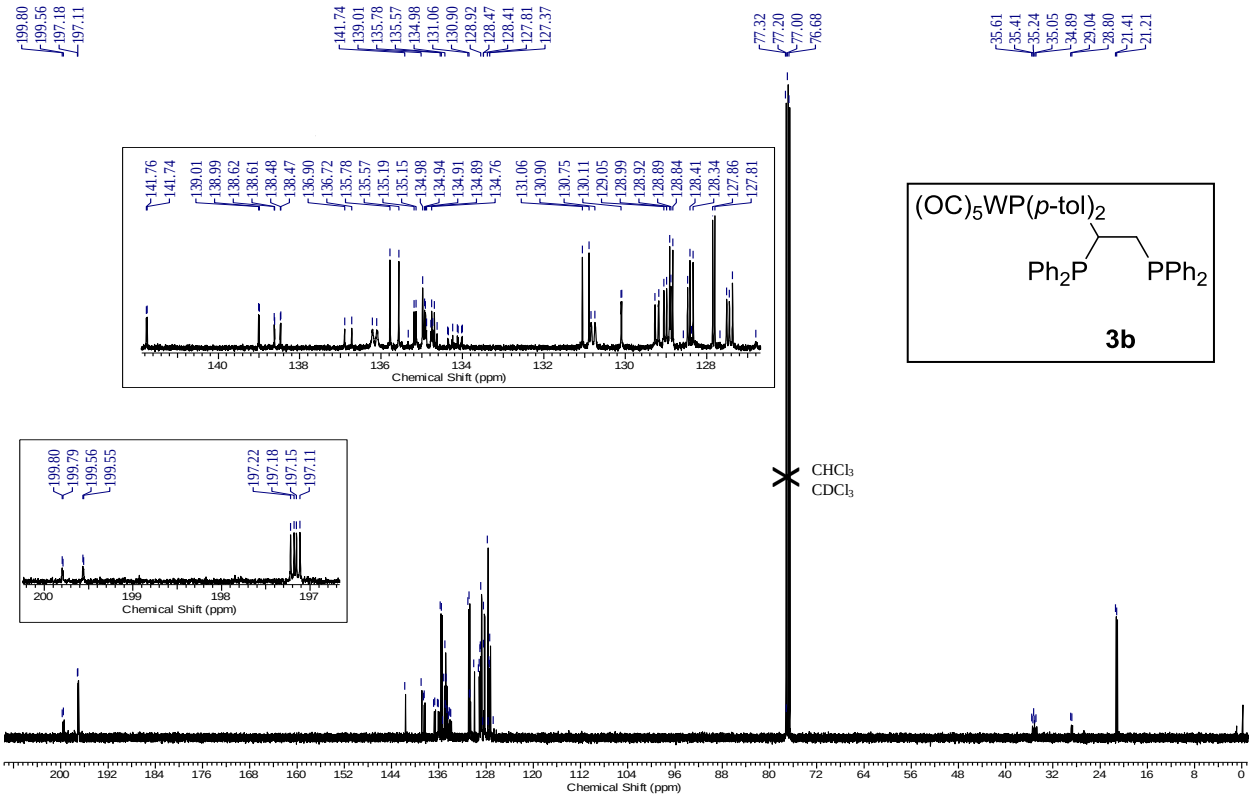

Figure S5.3. $^{13}C\{^1H\}$ NMR spectrum of $[(OC)_5W\{\kappa^1\text{-}P(p\text{-tol})_2CH(PPh_2)CH_2PPh_2\}]$ **3b**.

$^{31}P\{^1H\}$ NMR of mixture:

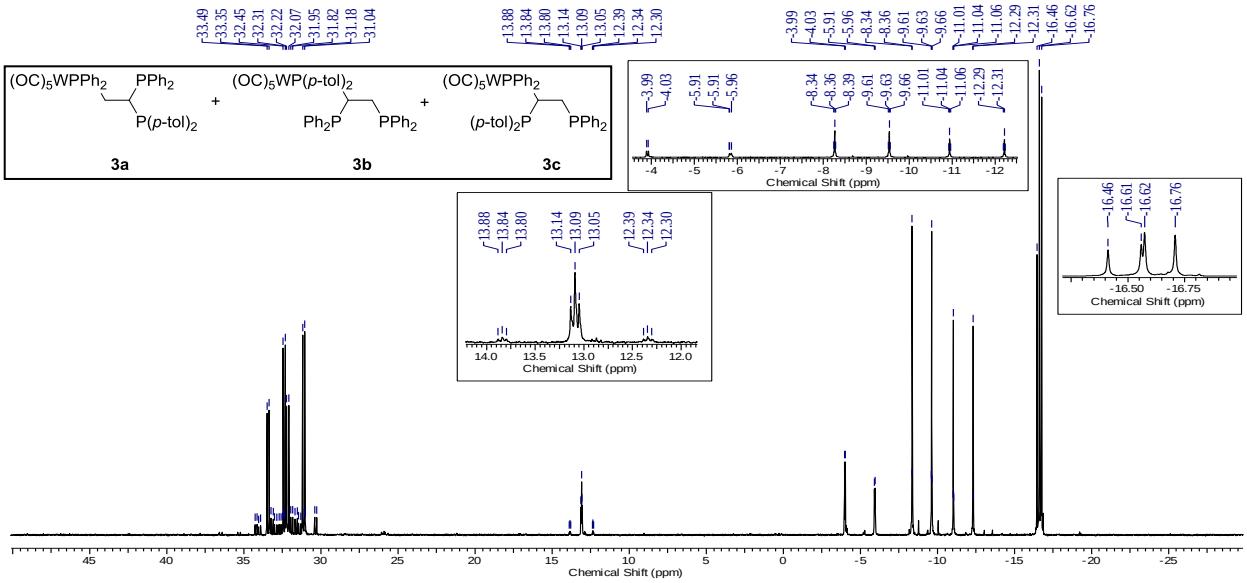

Figure S5.4 $^{31}P\{^1H\}$ NMR spectrum of mixture of $[(OC)_5W\{\kappa^1\text{-}PPh_2CH_2CH(PPh_2)[P(p\text{-tol})_2]\}]$ **3a**, $[(OC)_5W\{\kappa^1\text{-}P(p\text{-tol})_2CH(PPh_2)CH_2PPh_2\}]$ **3b**, and $[(OC)_5W\{\kappa^1\text{-}PPh_2CH[P(p\text{-tol})_2]CH_2PPh_2\}]$ **3c**

6. High-Resolution Mass spectrum of $[(OC)_5W\{\kappa^1\text{-}P(p\text{-tol})_2CH(PPh_2)CH_2PPh_2\}]$ 3b:

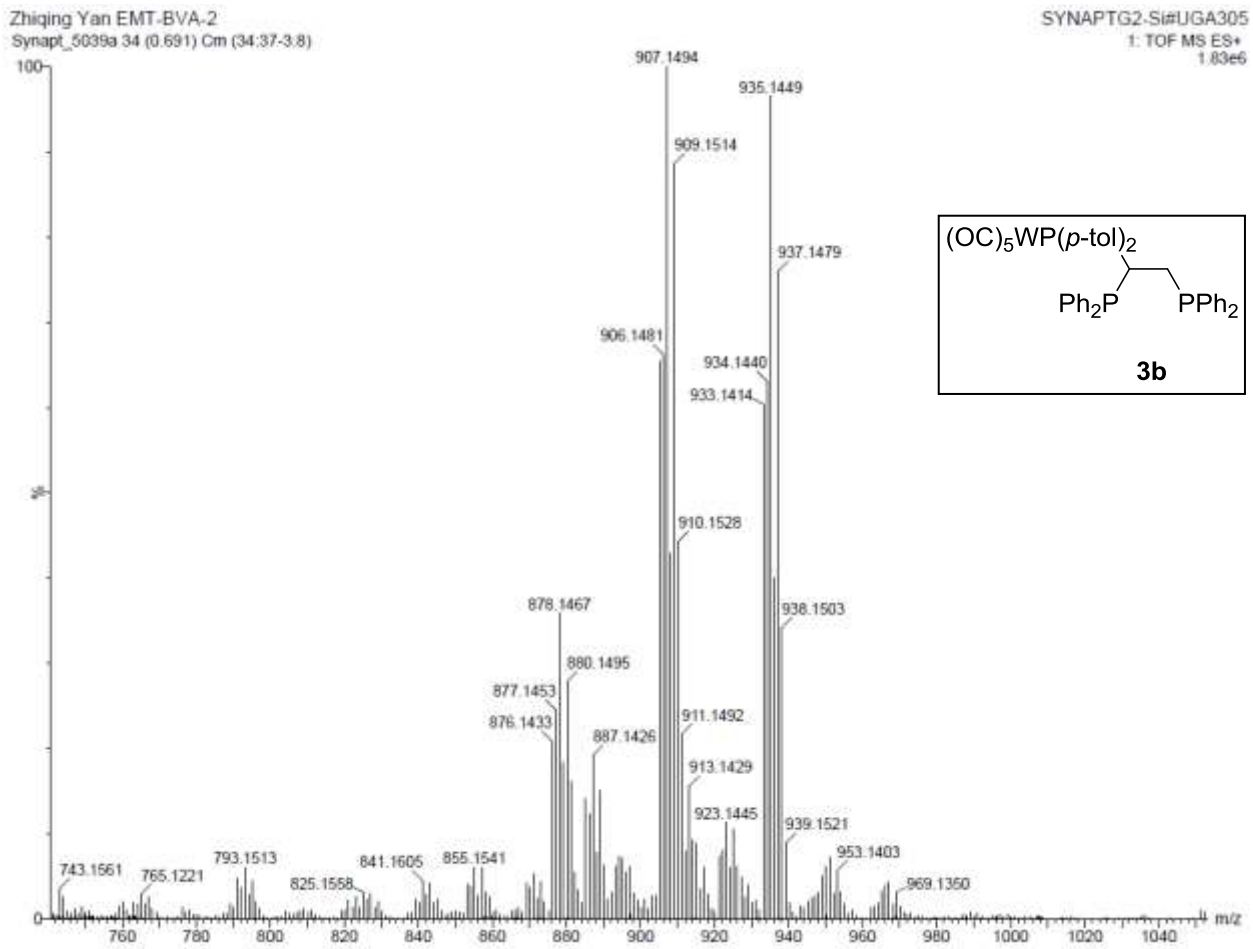

Elemental Composition Report

Single Mass Analysis
Tolerance = 5.0 PPM / DBE: min = -1.5, max = 150.0
Element prediction: Off
Number of isotope peaks used for i-FIT = 2

Monoisotopic Mass, Odd and Even Electron Ions
19 formula(e) evaluated with 1 results within limits (up to 10 best isotopic matches for each mass)
Elements Used:
C: 0-100 H: 0-180 O: 5-5 P: 3-3 184W: 0-1

Minimum:				-1.5				
Maximum:		5.0	5.0	150.0				
Mass	Calc. Mass	mDa	PPM	DBE	i-FIT	Norm	Conf(%)	Formula
935.1449	935.1441	0.8	0.9	30.0	242.7	n/a	n/a	C45 H38 O5 P3 184W

Figure S6.1. Mass spectrum of $[(OC)_5W\{\kappa^1\text{-}P(p\text{-tol})_2CH(PPh_2)CH_2PPh_2\}]$ **3b.**

7. IR spectrum of $[(OC)_5W\{\kappa^1\text{-}P(p\text{-tol})_2CH(PPh_2)CH_2PPh_2\}]$ 3b

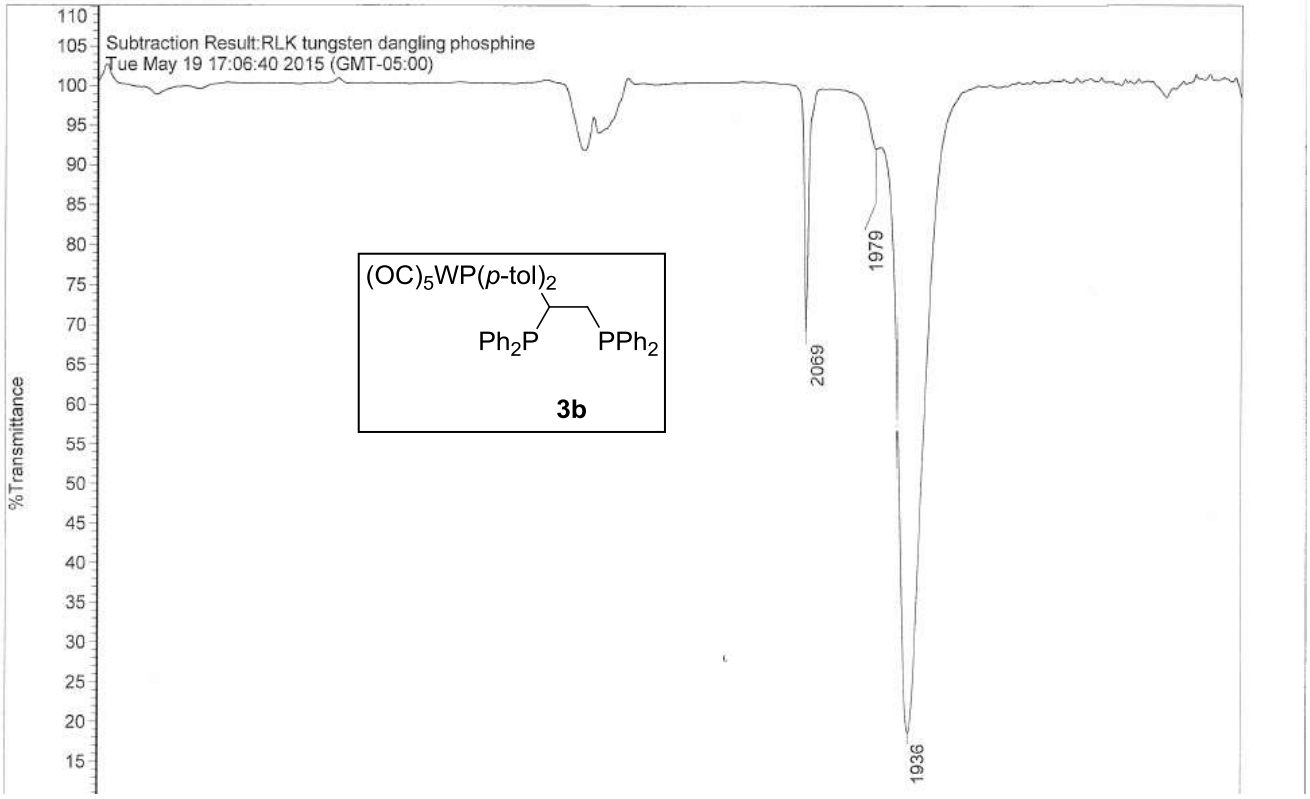

Figure S7.1. Carbonyl region of the IR spectrum of $[(OC)_5W\{\kappa^1\text{-}P(p\text{-tol})_2CH(PPh_2)CH_2PPh_2\}]$ **3b**.

8. Kinetic Analysis

The consecutive two-step reversible reaction of the form

$$A \underset{k_{-1}}{\overset{k_1}{\rightleftharpoons}} B \underset{k_{-2}}{\overset{k_2}{\rightleftharpoons}} C \tag{1}$$

has rate equations given by the following:

$$-\frac{d[A]}{dt} = k_1[A] - k_{-1}[B] \tag{2}$$

$$\frac{d[B]}{dt} = k_1[A] - k_{-1}[B] - k_2[B] + k_{-2}[C] \tag{3}$$

$$\frac{d[C]}{dt} = k_2[B] - k_{-2}[C] \tag{4}$$

Note that, for the purposes of this work, the conversion of isomer C to A is ignored. This is a valid assumption if the rate of inter-conversion of $A \longleftrightarrow C$ is small. Given the experimental data, a steady-state approximation for the system of rate equations is not valid for isomer B because its concentration is rather close to those of A and C and changes appreciably. Thus, the differential equations in (2)-(4) must be solved explicitly. The exact solutions to these equations are:

$$A(t) = A_0\left[\frac{k_{-1}k_{-2}}{mn} + \frac{k_1(m-k_2-k_{-2})}{m(m-n)} * e^{-mt} + \frac{k_1(k_2+k_{-2}-n)}{n(m-n)} * e^{-nt}\right] \tag{5}$$

$$B(t) = A_0\left[\frac{k_1k_{-2}}{mn} + \frac{k_1(k_{-2}-m)}{m(m-n)} * e^{-mt} - \frac{k_1(k_{-2}-n)}{n(m-n)} * e^{-nt}\right] \tag{6}$$

$$C(t) = A_0\left[\frac{k_1k_2}{mn} - \frac{k_1k_2}{m(m-n)} * e^{-mt} + \frac{k_1k_2}{n(m-n)} * e^{-nt}\right] \tag{7}$$

Where,

$$m = \frac{1}{2}(p+q) \tag{8}$$

$$n = \frac{1}{2}(p-q) \tag{9}$$

$$p = k_1 + k_{-1} + k_2 + k_{-2} \tag{10}$$

$$q = \left(p^2 - 4(k_1k_2 + k_{-1}k_{-2} + k_1k_{-2})\right)^{\frac{1}{2}} \tag{11}$$

The values of *m* and *n* generally differ by less than an order of magnitude within the range of rate constant values expected for Reaction (1). Thus, fits to time-dependent data in the form of $y(t) = y_0 + \Lambda e^{-\lambda t} + Ke^{-\kappa t}$ tend to converge to the form $y(t) = y_0 + \alpha e^{-\beta t}$. We take advantage of this to approximate k_1 by fitting data for isomer A with a single exponential such that equation (5) may be rearranged as:

$$A(t) = A_0\left[\frac{k_{-1}k_{-2}}{k_1k_2 + k_{-1}k_{-2} + k_1k_{-2}} + \left[\frac{k_1k_2 + k_1k_{-2}}{k_1k_2 + k_{-1}k_{-2} + k_1k_{-2}}\right] * e^{-x_1t}\right] \tag{12}$$

Similarly, the integrated rate laws for isomers B and C may be rewritten as:

$$B(t) = A_0 \left[\frac{k_1 k_{-2}}{k_1 k_2 + k_{-1} k_{-2} + k_1 k_{-2}} + \left[\frac{k_1 k_{-2}}{k_1 k_2 + k_{-1} k_{-2} + k_1 k_{-2}}\right] * e^{-x_2 t}\right] \quad (13)$$

$$C(t) = A_0 \left[\frac{k_1 k_2}{k_1 k_2 + k_{-1} k_{-2} + k_1 k_{-2}} + \left[\frac{k_1 k_2}{k_1 k_2 + k_{-1} k_{-2} + k_1 k_{-2}}\right] * e^{-x_3 t}\right] \quad (14)$$

Note that in equations (12) and (14), x_1 and x_3 are roughly equivalent to k_1 and k_{-2}, respectively. x_2 does not have an obvious analogue. At equilibrium, for a normalized data set, the following relations also hold:

$$1 = [A] + [B] + [C] \quad (15)$$

$$[A] = \frac{k_{-1}}{k_1}[B] = \frac{1}{K_1}[B] \quad (16)$$

$$[C] = \frac{k_2}{k_{-2}}[B] = K_2[B] \quad (17)$$

Where K_1 and K_2 are the equilibrium constants for the first and second step of Reaction (1), respectively. Substituting Eqns (16) and (17) into (15) and rearranging yields the following relationship:

$$[B]_e = \frac{k_1 k_{-2} A_0}{k_1 k_2 + k_{-1} k_{-2} + k_1 k_{-2}} \quad (18)$$

Then, in solving for Eqn (2) at equilibrium,

$$\frac{d[A]}{dt} = \frac{k_1 k_{-1} k_{-2}}{k_1 k_2 + k_{-1} k_{-2} + k_1 k_{-2}} + \frac{k_1 k_{-1} + k_1 k_{-2}}{k_1 k_2 + k_{-1} k_{-2} + k_1 k_{-2}} * e^{-k_1 t} \quad (19)$$

Thus, by inspection of Eqns (12) and (19), $x_1 \approx k_1$. Equation (4) may be similarly rearranged and integrated to solve assuming equilibrium conditions, where $x_3 \approx k_{-2}$. Unfortunately, equations (12)-(14) cannot be expressly used to determine exact values for k_1, k_{-1}, k_2, and k_{-2} explicitly because those variables are coupled (recall the simplifying assumption that a three-component exponential fit to the experimental data converges to a two-component exponential fit when values of m and n are similar). It is, however, relatively straightforward to determine K_1 and K_2 by fitting the experimental data with a function of the form $y(t) = y_0 + \alpha e^{-\beta t}$ to obtain y_0 and β for A, B, and C at each temperature. It then follows that

$$K_1 = \frac{y_o(B)}{y_o(A)} \quad (20)$$

and

$$K_2 = \frac{y_o(C)}{y_o(B)} \quad (21)$$

Finally, K_1 and K_2 may be used to estimate the remaining two unknowns, k_{-1}, k_2, from the estimated values of k_1, and k_{-2}.

9. Graphs of NMR Intensities vs Time for all Four Temperatures

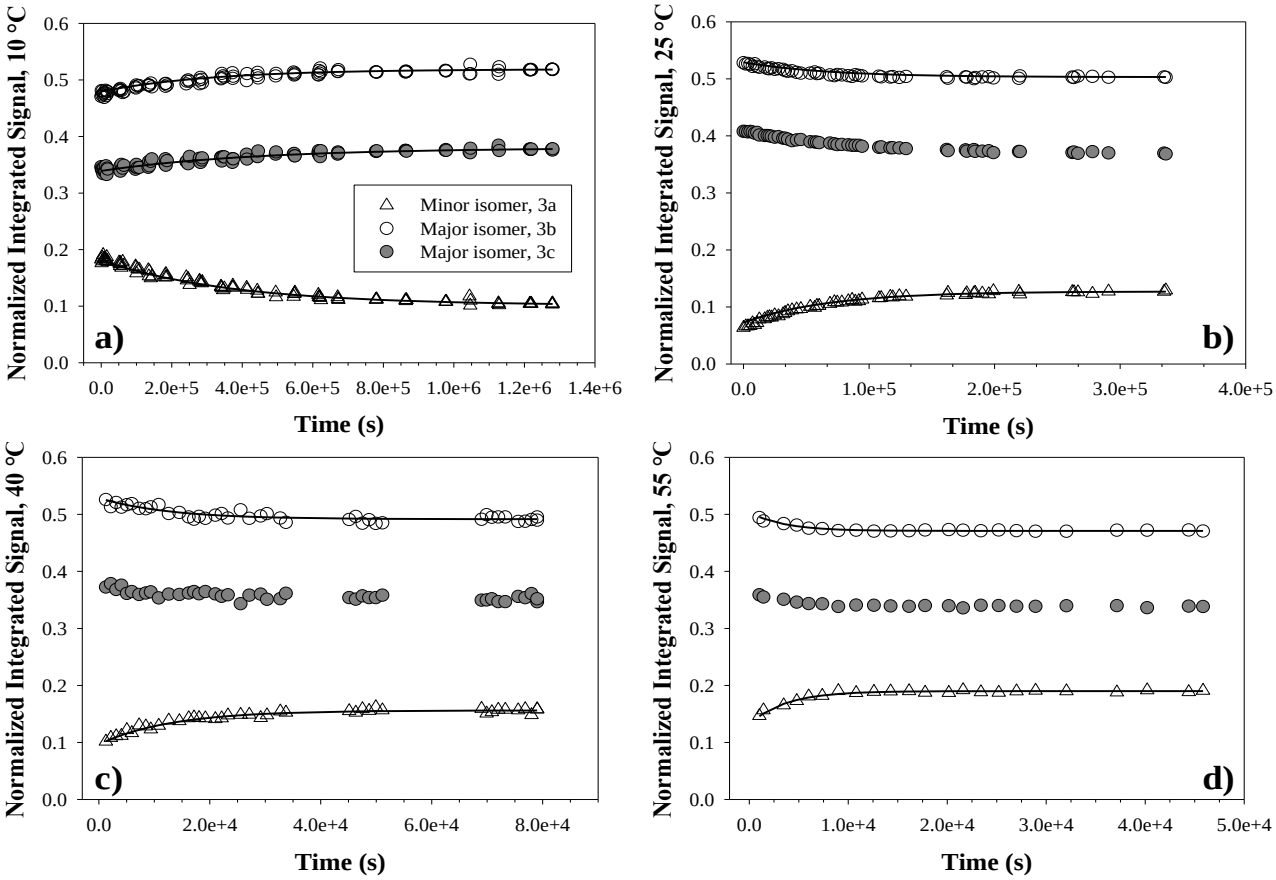

Figure S8. Normalized NMR signal intensities as a function of elapsed experiment time at four temperatures: a) 10, b) 25, c) 40, d) 55˚C. Empty circles correspond to the major isomer **3b**, the filled circles to the major isomer **3c**, and triangles to the minor isomer **3a**. Overlaid solid lines show the time dependence of each isomer at each temperature and are calculated from the integrated rate laws using the four rate constants determined by this work.

10. Crystallographic data for $[(OC)_5W[\{\kappa^1\text{-}P[(p\text{-tol})_2]CH(PPh_2)CH_2PPh_2\}]$ 3b

Table S8.1 Crystallographic data for $[(OC)_5W[\{\kappa^1\text{-}P[(p\text{-tol})_2]CH(PPh_2)CH_2PPh_2\}]$ **3b**

Crystal data	
CCDC deposit no.	1849765
Empirical formula	$C_{45}H_{37}O_5P_3W$
Crystal System, space group	Monoclinic $P2_1/n$
M_r	934.50
a, Å	13.5542(3)
b, Å	13.4842(3)
c, Å	22.5748(4)
α, deg	90
β, deg	104.841(1)
γ, deg	90
V, (Å^3)	3988.30(14)
Z, Z'	4, 1
D_{calc} (g cm^{-3})	1.556
μ (mm^{-1}), rad. type	6.873, Cu $K\alpha$
F_{000}	1864
temp (K)	100(2)
Crystal form, color	rhomboid, colorless
Crystal size, mm	0.11 x 0.13 x 0.14
Data collection	
Diffractometer	Bruker Apex II
T_{min}/ T_{max}	0.484 / 0.753
No. of refls. (meas., uniq., and obs.)	57132, 7297, 6720
R_{int}	0.0552
θ_{max} (^{o})	68.24
Refinement	
R/R^2_ω (obs data)	0.0280 / 0.0700
R/R^2_ω (all data)	0.0310 / 0.0719
S	1.04
No. of refls.	7297
No. of parameters	489
$\Delta\rho_{max/min}$ (e·Å^{-3})	0.613 / -0.242
Flack x	-